# Nickel(IV)-Catalyzed C-H Trifluoromethylation of (Hetero)arenes

Elizabeth A. Meucci,<sup>†</sup> Shay N. Nguyen,<sup>†</sup> Nicole M. Camasso,<sup>†</sup> Eugene Chong,<sup>†</sup> Alireza Ariafard,<sup>‡</sup> Allan J. Canty,<sup>‡</sup> and Melanie S. Sanford\*,<sup>†</sup>

<sup>†</sup>Department of Chemistry, University of Michigan, 930 N University Ave, Ann Arbor, MI 48109, USA <sup>§</sup>School of Physical Sciences, University of Tasmania, Hobart, Tasmania 7001, Australia

ABSTRACT: This Article describes the development of a stable Ni<sup>IV</sup> complex that mediates C(sp<sup>2</sup>)–H trifluoromethylation reactions. This reactivity is first demonstrated stoichiometrically and then successfully translated to a Ni<sup>IV</sup>-catalyzed C–H trifluoromethylation of electron-rich arene and heteroarene substrates. Both experimental and computational mechanistic studies support a radical chain pathway involving Ni<sup>IV</sup>, Ni<sup>III</sup>, and Ni<sup>II</sup> intermediates.

Supporting Information Placeholder

#### INTRODUCTION

Over the past three decades, nickel has emerged as an economical base-metal catalyst for a wide array of important chemical transformations.1 The vast majority of these Ni-catalyzed processes are proposed to proceed via Ni<sup>0/II</sup>, Ni<sup>1/III</sup> or Ni<sup>1/IIII</sup> catalytic cycles.<sup>2</sup> In many cases, these mechanisms are supported by the isolation of organonickel intermediates and studies of their catalytic competence.<sup>3</sup> While organonickel(I), (II), and (III) complexes are well-precedented, until 5 years ago there were very few examples of isolable Ni complexes in the +4 oxidation state.<sup>4</sup> As a result, Ni<sup>IV</sup> intermediates have rarely been proposed in catalysis. However, recent progress by our group and others has shown that organonickel(IV) complexes can be synthesized at room temperature using mild oxidants. 4b-e Given the accessibility and unique reactivity of Ni<sup>IV</sup>, we sought to investigate its relevance in catalysis.

Ni<sup>IV</sup>–CF<sub>3</sub> complexes have been shown to exhibit superior stability when compared to other Ni<sup>IV</sup>–alkyls.<sup>5</sup> They are also easily prepared via the net two-electron oxidation of Ni<sup>II</sup> precursors with CF<sub>3</sub>+ oxidants (for example, see **A** in Figure 1A).<sup>4,5</sup> Additionally, a recent report by Nebra and coworkers demonstrated a Ni<sup>IV</sup>–CF<sub>3</sub> complex that effects the stoichiometric C–H trifluoromethylation of 1,2-dichlorobenzene under mild conditions (Figure 1B).<sup>6</sup> Inspired by these results, we hypothesized that we could develop a Ni<sup>IV</sup>-catalyzed method for the C–H trifluoromethylation of arenes by identifying the optimal combination of ligand, substrate, and CF<sub>3</sub>+ oxidant (Figure 1C).

We demonstrate herein the design and synthesis of a  $Ni^{IV}$ – $CF_3$  complex that participates in a net transfer of  $CF_3$ <sup>+</sup> to electron-rich arenes. Furthermore, in the presence of an electrophilic trifluoromethylating reagent, this  $Ni^{IV}$  complex serves as an effective catalyst for the C–H trifluoromethylation of arene and heteroarene substrates.

Mechanistic studies suggest that this reaction proceeds through a  $Ni^{II/III/IV}$  cycle involving  $CF_3$  radicals as key intermediates.

A. Sanford 2015: Stoichiometric synthesis of Ni<sup>IV</sup>–CF<sub>3</sub> complexes

$$(A)$$

$$(A)$$

$$(B)$$

$$(A)$$

$$(B)$$

$$(A)$$

$$(B)$$

$$(A)$$

$$(B)$$

$$(B)$$

$$(B)$$

$$(CF_3)$$

$$(CF_3)$$

B. Nebra 2017: Stoichiometric CF<sub>3</sub> transfer from Ni<sup>IV</sup>–CF<sub>3</sub> complexes

C. This work:  $Ni^{IV}$ – $CF_3$  catalyzed C–H trifluoromethylation

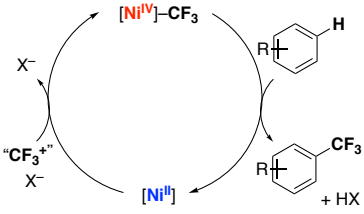


**Figure 1.** (A) Synthesis of  $Ni^{IV}$ – $CF_3$  complexes. (B) Stoichiometric  $C(sp^2)$ –H trifluoromethylation mediated by  $Ni^{IV}$ . (C) Overall cycle for  $Ni^{IV}$ -catalyzed trifluoromethylation.

# RESULTS AND DISCUSSION

Design and synthesis of Ni<sup>IV</sup>–CF<sub>3</sub> complex. Our initial efforts focused on identifying a ligand scaffold that would enable both steps of the proposed catalytic cycle: (1) the net 2e<sup>-</sup> oxidation of a Ni<sup>II</sup> precursor with a "CF<sub>3</sub>+" oxidant to afford a Ni<sup>IV</sup>–CF<sub>3</sub> complex and (2) the subsequent reaction of this Ni<sup>IV</sup>–CF<sub>3</sub> with arenes to afford C(sp<sup>2</sup>)–H trifluoromethylation products. Based on previous work from our group,<sup>4c,5a</sup> we hypothesized that the tris(pyrazolyl)borate (Tp) ligand would be effective in this context. Furthermore, based on Nebra's results,<sup>6</sup> we

reasoned that the incorporation of multiple  $CF_3$  ligands would render the resulting complex reactive towards  $CF_3$  transfer reactions. With these considerations in mind, we initially targeted  $TpNi^{IV}(CF_3)_3$  (II) (eq. 1).

Complex **II** was synthesized via the oxidation of Ni<sup>II</sup> complex **I** with 2,8-difluoro-5-(trifluoromethyl)-5*H*-dibenzo[*b,d*]thiophen-5-ium trifluoromethanesulfonate (**B**). The Ni<sup>IV</sup> product was isolated in 47% yield as a yellow solid and was characterized by <sup>1</sup>H, <sup>19</sup>F, <sup>13</sup>C, and <sup>11</sup>B NMR spectroscopy. X-ray quality crystals were obtained by recrystallization from MeCN, and an ORTEP diagram is shown in Figure 2.

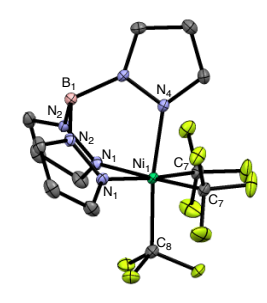


**Figure 2.** ORTEP diagram for complex **II**. Hydrogen atoms have been omitted for clarity, thermal ellipsoids drawn at 50% probability. Bond lengths (Å):  $Ni_1-N_1=2.013$ ,  $Ni_1-N_4=1.974$ ,  $Ni_1-C_7=2.011$ ,  $Ni_1-C_8=1.983$  and bond angles (deg):  $C_7-Ni_1-C_7=99.81$ ,  $C_7-Ni_1-C_8=88.05$ .

In the solid state, complex **II** is extremely stable to ambient conditions, showing no signs of decomposition after more than a year of storage on the benchtop. However, under analogous conditions as a 0.01 M solution in MeCN, **II** begins to decompose within 72 h at room temperature. Over this time, the NMR resonances associated with complex **II** gradually disappear, along with concomitant formation of CF<sub>3</sub>H.

We next explored the reactivity of **II** in stoichiometric C(sp²)–H trifluoromethylation. Initial studies focused on 1,2-dichlorobenzene (1), the substrate originally employed by Nebra (Scheme 1B).<sup>6</sup> As shown in Table 1, entry 1, the reaction of **II** with 1 equiv of 1 afforded traces (<5%) of the C–H trifluoromethylation product 1-CF<sub>3</sub> after 24 h at room temperature. This yield increased to 9% when **1** was used as the reaction solvent under otherwise analogous conditions (Table 1, entry 2). We next examined the more electron rich substrate 1,3,5-trimethoxybenzene (2). As shown in Table 1, entry 3, complex **II** reacted with 1 equiv of **2** to afford **2-CF**<sub>3</sub> in 47% yield as determined by <sup>19</sup>F NMR spectroscopic analysis of the crude reaction mixture. The Ni<sup>II</sup> product **I-H**<sup>+</sup> was also formed in 56% yield.<sup>7</sup> These yields increased to 72% and

74%, respectively, upon the use of 5 equiv of 1,3,5-trimethoxybenzene relative to  $\mathbf{H}$ .

Table 1. Reactions of II with Ar-H substrates.

<sup>a</sup>Yields determined by <sup>19</sup>F NMR spectroscopy using trifluorotoluene as an internal standard and are based on **II**. All reactions conducted using 1.0 equiv **II**.  $^{b}1:1.2$  ratio of **1-CF**<sub>3</sub>**isomers**.

Finally, we evaluated the feasibility of regenerating Ni<sup>IV</sup> complex **II** via the oxidation of **I-H**<sup>+</sup> with **B**. As shown in eq. 2, the treatment of a solution of **I-H**<sup>+</sup> (generated *in situ* from the reaction of **II** with **2**) with 1.5 equiv of **B** afforded **II** in 63% yield after 30 s. Overall, thees studies demonstrate each individual step in the **II**-catalyzed trifluoromethylation of **2**.

Complex II-catalyzed C-H trifluoromethylation. We next explored the use of II as a catalyst for the C-H trifluoromethylation of arenes using **B** as the "CF<sub>3</sub>+" source.8,9 Initial studies employed 5 mol % of II in combination with 1 equiv of 1,3,5-trimethoxybenzene and 1 equiv of **B** in DMSO. After 24 h at room temperature in the dark, this reaction afforded 37% yield of the C-H trifluoromethylation product 2-CF<sub>3</sub> (Table 2, entry 1). Importantly, no reaction was observed in the absence of complex II under these conditions (Table 2, entry 2). The presence/absence of ambient light did not impact the yield, ruling out a photoredox-type pathway (Table 2, entries 1 and 3). Employing complex I as the catalyst resulted in slightly diminished yield (25%, entry 4). The use of A as an oxidant also afforded a lower yield (25%, entry 5). Employing an excess of 2 (2 or 5 equiv relative to **B**) led to an increase in the yield of product 2-CF<sub>3</sub> (to 62% and 93%, respectively, entries 6 and 7). Optimization of the reaction time, concentration, temperature, and solvent revealed that the highest yield of **2-CF**<sub>3</sub> (93%) is obtained under the conditions in entry 7 (see SI for complete optimization details).

Table 2. Optimizing Ni<sup>IV</sup>-catalyzed trifluoromethylation

entry	modification	yield (%)a
1	dark	37
2	no <b>II</b>	0
3	ambient light	35
4	I as catalyst	25
5	A used as oxidant	25
6	2 equiv substrate	62
7	5 equiv substrate	93

 $<sup>^</sup>a\overline{Y}$ ields determined by  $^{19}F$  NMR spectroscopy using trifluorotoluene as an internal standard and are based on **B** as the limiting reagent. Standard conditions: 1.0 equiv **2**, 1.0 equiv **B**, 5 mol% **II** in DMSO at room temperature for 24 h.

**Scheme 1.** Scope of Ni<sup>IV</sup>-catalyzed trifluoromethylation<sup>a</sup>

We next evaluated the scope of this **II**-catalyzed C—H trifluoromethylation. As shown in Scheme 1, this reaction proved applicable to a variety of electron-rich arene and heteroarene substrates (Scheme 1). In addition to trimethoxybenzene, electron rich pyridines as well as indole and thiophene derivatives showed good reactivity. A variety of biologically active molecules, including melatonin, Boc-L-tryptophan, resorcinol, and tadalafil, also

served as effective substrates for this transformation. Notably, trifluoromethylation of tadalafil occurs at the 7-position of the indole backbone (rather than on the 1,3-dioxole-substituted ring), a site that has been functionalized in several other reported radical trifluoromethylation reactions. Overall, this transformation works best with highly electron-rich (hetero)arenes, while less electron rich substrates afforded moderate to low yields (see SI for details of other substrates examined). This relatively narrow substrate scope as well as the use of 5 equiv of (hetero)arene substrate relative to oxidant represent limitations of this method compared to state-of-the-art radical C–H trifluoromethylation protocols.

Scheme 2. Two possible mechanisms for CF<sub>3</sub> transfer from II

$$\begin{array}{c} H \\ CF_3 \\ HB \\ N \\ N \\ N \\ CF_3 \\ CF_3 \\ (II) \end{array} + R \\ \begin{array}{c} H \\ (I3) \\ \hline \\ (I3) \\ \hline \\ (I4) \\ \hline \\ (I5) \\ \hline \\ (I6) \\ \hline \\ (I6) \\ \hline \\ (I6) \\ \hline \\ (I7) \\ \hline \\ (I8) \\ \hline \\ (I7) \\ \hline \\ (I8) \\ \hline \\ (I7) \\ \hline \\ (I7) \\ \hline \\ (I8) \\ \hline \\ (I7) \\ \hline \\ (I8) \\ \hline \\ (I7) \\ \hline \\ (I8) \\ \hline \\ (I7) \\ \\ (I7) \\ \hline \\ (I7) \\ \\$$

To gain further insights into this transformation, we first conducted a time study, monitoring the consumption of **II** and appearance of **2-CF**<sub>3</sub> via <sup>19</sup>F NMR spectroscopy. As shown in Figure 3, an induction period of approximately 25 min is observed, followed by rapid consumption of starting material and concomitant appearance of **2-CF**<sub>3</sub>. This reaction profile provides initial evidence against a direct transfer of CF<sub>3</sub><sup>+</sup> from **II** (Scheme 2, i), as no induction period would be expected for this pathway.

 $<sup>^</sup>a$  General conditions: 1.0 equiv **B**, 5.0 equiv arene, 5 mol % of **II** in DMSO for 24 h at 25 °C. <sup>19</sup>F NMR yields are in parentheses and were determined using trifluorotoluene as an internal standard. In cases where multiple isomers were formed, NMR yield is given as a combined yield. \*Signifies the site of a minor isomer.

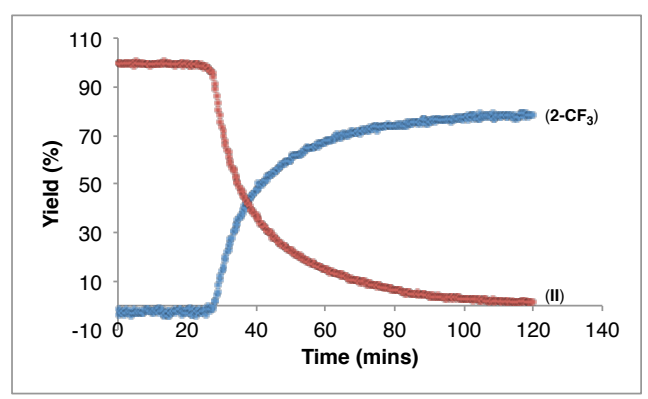


**Figure 3.** Reaction profile for the trifluoromethylation of trimethoxybenzene with complex **II**. Reaction conducted with 1.0 equiv **II** and 5.0 equiv **2**.

Reaction profiles like that in Figure 3 are characteristic of radical chain processes.<sup>13</sup> To trap putative radical intermediates, we next carried out the reaction between **II** and **2** in the presence of TEMPO. As shown in eq. 3, the addition of 1 equiv of TEMPO inhibited productive C–H trifluoromethylation, decreasing the yield of **2-CF**<sub>3</sub> from 72% to just 4% under otherwise analogous conditions. Furthermore, TEMPO–CF<sub>3</sub> (**15**, 8%) was detected by <sup>19</sup>F NMR spectroscopy.<sup>14</sup>

The diminished yield of 2-CF<sub>3</sub> and observation of 15 in the presence of TEMPO both implicate the intermediacy of CF<sub>3</sub>• in this transformation. Based on the mechanism in Scheme 2, ii, this could be accompanied by the formation of the Ni<sup>III</sup> intermediate III, a species that we have independently synthesized and characterized by EPR spectroscopy in a 3:1 mixture of PrCN:MeCN.<sup>15</sup> To test for the formation of III, we conducted the reaction between II and 2 and removed aliquots at several time points before, during, and after the induction period (0.5. 35, 45, and 85 min). The samples were then diluted in PrCN, and EPR spectra were acquired for each time point. As shown in Figure S45, signals consistent with a Tp-ligated Ni<sup>III</sup> intermediate are observed; however, the EPR data for the major species present in these samples do not match those for III. This suggests that the major Ni<sup>III</sup> species formed under these conditions is not complex III. Furthermore, as shown in eq. 3, the addition of 1 equiv of III to the reaction between II and 2 inhibited the formation of 2-CF<sub>3</sub>, with none of the product observed after 45 min. 16 Overall, these data suggest that complex III is not the major Ni<sup>III</sup> intermediate formed under these conditions.

Based on these studies, we propose a radical chain mechanism for the **II**-mediated C–H trifluoromethylation of **2**. As shown in Scheme 3, i, the radical chain initiates via slow Ni<sup>IV</sup>–CF<sub>3</sub> bond homolysis. This liberates CF<sub>3</sub>•, which then enters the chain propagation sequence (Scheme 3, ii). Propagation is proposed to involve: (1) reaction of CF<sub>3</sub>• with **2** to afford intermediate **14**; (2) oxidation and deprotonation of **14** by Ni<sup>IV</sup> complex **II** to generate a protonated Ni<sup>III</sup> intermediate **IV**; and (3) Ni<sup>III</sup>–CF<sub>3</sub> homolysis from **IV** to release **I-H**<sup>+</sup> and regenerate CF<sub>3</sub>•. Importantly, the 17-electron Ni<sup>III</sup> complex **IV** is expected to be more reactive towards Ni–CF<sub>3</sub> bond homolysis than the neutral, 18-electron Ni<sup>IV</sup> starting material **II**.<sup>17</sup> This should render chain propagation faster than initiation, resulting in a reaction profile like that in Figure 3.

**Scheme 3.** Proposed radical chain pathway for **II**-mediated C–H trifluoromethylation

(3) 
$$N_{1}^{\parallel \parallel}$$
  $CF_{3}$   $C$ 

If the mechanism in Scheme 3 is operative, then the induction period should be eliminated if the protonated (tris)trifluoromethyl Ni<sup>III</sup> complex **IV** is generated independently. Based on the cyclic voltammogram of **4** (Figure S52), Cp<sub>2</sub>Co ( $E_{1/2} = -1.33$  V vs SCE) should effect the single electron reduction of **II** ( $E_{1/2} = -0.395$  V vs SCE). In the presence of 1 equiv of TsOH•H<sub>2</sub>O, this is

expected to afford **IV**, thus chemically initiating the reaction (Scheme 4).<sup>18</sup>

Scheme 4. Reduction of II as a route to CF<sub>3</sub>•

$$(II) \xrightarrow{Cp_2Co} \underset{TSOH \cdot H_2O}{\overset{\bigcirc}{HB}} \underset{V}{\overset{\bigcirc}{N}} \underset{N}{\overset{\bigcirc}{N}} \underset{CF_3}{\overset{\bigcirc}{N}} \underset{CF_3}{\overset{\bigcirc}{HB}} \underset{V}{\overset{\bigcirc}{N}} \underset{N}{\overset{\bigcirc}{N}} \underset{N}{\overset{\bigcirc}{N}} \underset{CF_3}{\overset{\bigcirc}{N}} + \underbrace{\cdot CF_3}$$

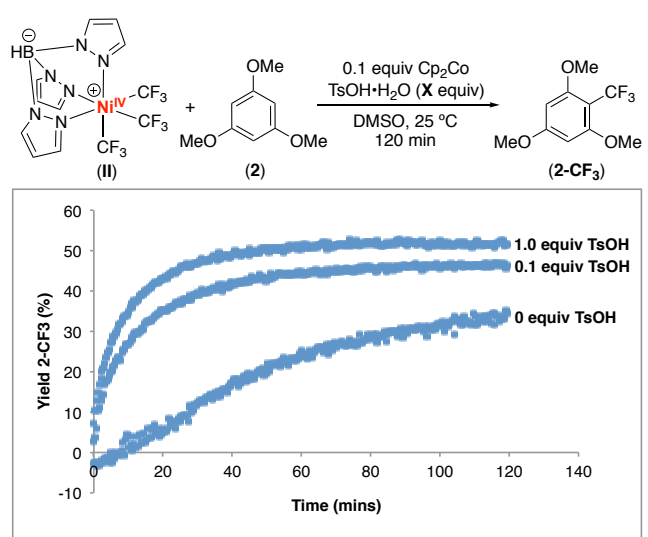
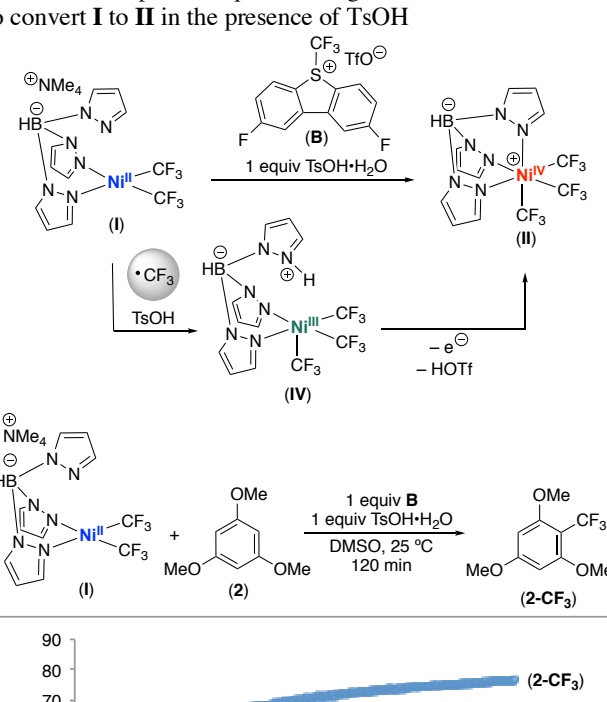
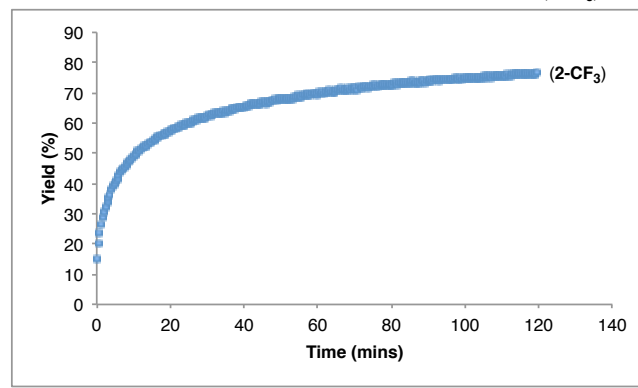


Figure 4. Reaction profile for the trifluoromethylation of trimethoxybenzene with complex II in the presence of Cp<sub>2</sub>Co and TsOH. Reaction conducted with 1.0 equiv II, 5.0 equiv 2, 0.1 equiv Cp<sub>2</sub>Co, and varied equiv of TsOH•H<sub>2</sub>O. Cp<sub>2</sub>Co was added to II and 2 immediately before the addition of TsOH•H<sub>2</sub>O.

It was recently reported that the generation of Ni<sup>IV</sup> complexes through the net 2-electron oxidation of Ni<sup>II</sup> precursors can proceed via two sequential one-electron oxidations involving the formation of transient Ni<sup>III</sup> intermediates.<sup>20</sup> If complex **II** were generated from **I** under acidic conditions via this type of pathway, Ni<sup>III</sup> species **IV** would be a likely intermediate (Scheme 5). We explored this possibility by examining the time course of **2-CF**<sub>3</sub> formation, using a combination of 1 equiv of Ni<sup>II</sup> complex **I**, 1 equiv of **B**, and 1 equiv TsOH•H<sub>2</sub>O to mediate the C–H trifluoromethylation of **2**. As shown in Figure 5, using **I/B/TsOH**, the reaction showed no induction period, and **2-CF**<sub>3</sub> was formed in 70% yield within 1 h at room temperature.

**Scheme 5.** Proposed sequential single electron oxidation step to convert **I** to **II** in the presence of TsOH





**Figure 5.** Reaction profile for the trifluoromethylation of trimethoxybenzene meditated by complex **I** in the presence of **B** and TsOH. Reaction conducted with 1.0 equiv **I**, 5.0 equiv **2**, 1.0 equiv **B**, and 1.0 equiv TsOH $\bullet$ H<sub>2</sub>O. **B** was added to **I** and **2** immediately before the addition of TsOH $\bullet$ H<sub>2</sub>O.

The results in Figure 5 can be rationalized based on the formation of the protonated Ni<sup>III</sup> intermediate **IV** during oxidation of **I**. We propose that **IV** then rapidly expels CF<sub>3</sub>• to initiate the reaction and enter the propagative cycle. However, notably, our proposed mechanism also implicates the intermediacy of Ni<sup>IV</sup> complex **II**, which serves as an oxidant during propagation. Consistent with this proposal, <sup>19</sup>F NMR spectroscopic monitoring of the trifluoromethylation of **2** with **I/B** showed that the Ni largely rests as Ni<sup>IV</sup> complex **II** during this transformation (Figure S48). This Ni<sup>IV</sup> complex persists throughout the product-forming stage, decaying at a rate that is similar to the rate of **2-CF**<sub>3</sub> formation. These results are mirrored in the catalytic variant of this reaction (see SI for details).

DFT studies of CF<sub>3</sub> transfer from complex II. We next examined the feasibility of the proposed pathway using DFT calculations.<sup>21</sup> Gaussian 09 was used at the B3LYP<sup>22</sup> level of density functional theory (DFT) for geometry optimization (see SI for complete details). Figure

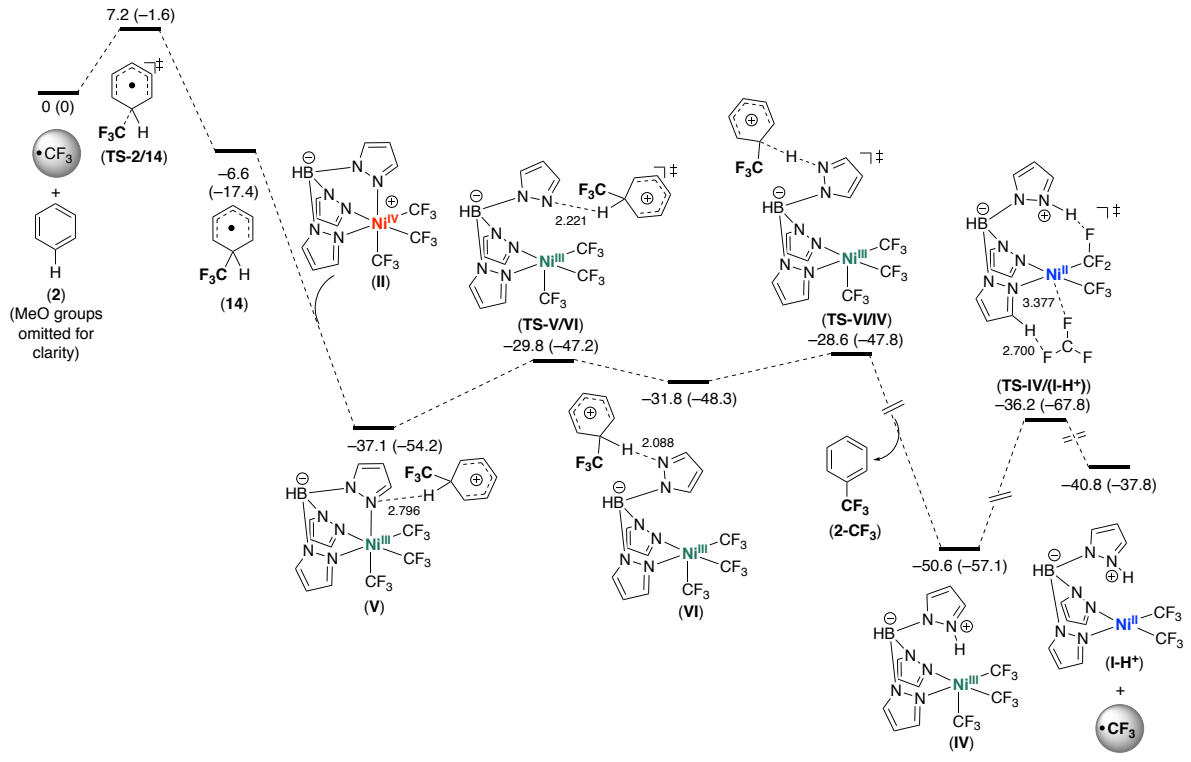


**Figure 6.** Energy profile for the propagation steps in the reaction of TpNi<sup>IV</sup>(CF<sub>3</sub>)<sub>3</sub> (II) with 1,3,5-trimethoxybenzene (2). Methoxy groups are omitted for clarity. Details for additional species: adduct after **TS-VI/IV** (-48.8 (-67.3)), conformer after **IV** formed by pyrazole rotation (-46.9 (-55.0), and adduct after **VII** (-36.1 (-40.7)) are provided in Supporting Information. Distances for selected interactions are given in Å. Energies  $\Delta G$  ( $\Delta H$ ) in kcal/mol are relative to ( $CF_3 \cdot + 2$ ).

6 illustrates the energy profile for propagation obtained following the initiation step that forms CF<sub>3</sub> radical.

The addition of CF<sub>3</sub>• to 2 to afford 14 is downhill by -6.6 kcal/mol (with  $\Delta G^{\dagger} = 7.7$  kcal/mol). The organic radical 14 exhibits a distorted tetrahedral geometry at the "C(H)(CF<sub>3</sub>)C<sub>2</sub>" center. As anticipated for  $\pi$ -delocalization, the C-C<sub>ortho</sub> bonds are ~0.1 Å longer than those between the other carbon atoms, and the SOMO exhibits  $\pi$ character located on these carbon and adjacent oxygen atoms. Compound 14 can undergo a highly favorable  $[\Delta G]$  $(\Delta H) = -30.5 (-36.8)$  kcal/moll electron transfer with Ni<sup>IV</sup> complex II to afford the arenium/NiII pair V in a barrierless process. Structure V exhibits a weak interaction between the organic fragment and a nitrogen atom coordinated to Ni (N····H = 2.796 Å). Spin density for V is located primarily at Ni (0.82 e/Å<sup>3</sup>), and the SOMO is an antibonding orbital located in the Ni coordination sphere (Figure 7). This is consistent with electron transfer from 14 to nickel to give Ni<sup>III</sup> and an arenium fragment.

The sequence  $V \rightarrow IV$  was obtained by initially locating transition state TS-VI/IV, followed by potential energy scans and optimizations from this structure. Notably, barriers within this sequence are very low:  $\Delta G^{\ddagger} = 3.2$  and 7.3 kcal/mol). Dissociation of the axial pyrazole occurs via transition state TS-V/VI to give VI, followed by proton transfer via transition state TS-VI/IV to afford a weak adduct that dissociates to form organic product 2- $CF_3$  and square-pyramidal  $Ni^{III}$  (IV). Consistent with the formulation of IV as a  $Ni^{III}$  complex, spin-density is

located primarily at Ni (Ni 0.68 e/ų,  $C_{axial}$  0.28 e/ų) and a LUMO can be readily assigned as Ni–C  $\sigma^*$  (Figure 7). Computation for loss of  $CF_3$ • from IV to give the diamagnetic Ni<sup>II</sup> product I-H+ led to detection of transition state TS-IV/I-H+ for  $CF_3$ • dissociation.

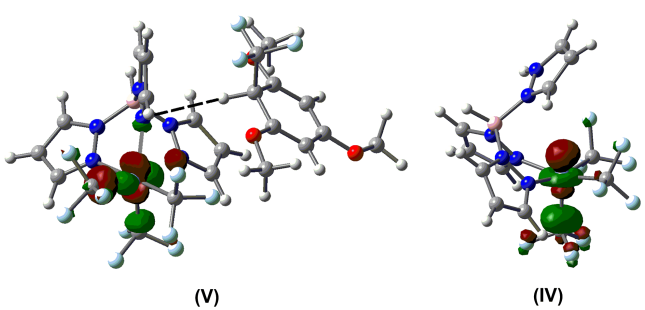


**Figure 7.** Nickel-centered SOMOs for **V** and **IV**, illustrating nickel-centered antibonding character in both structures.

Overall, these calculations show that the proposed steps of the propagative sequence have low barriers (<14.4 kcal/mol for  $IV \rightarrow I-H^+$ ) and are thus expected to be fast at 25 °C. We next turned our focus on the initiation step. A transition state for the formation of TpNi<sup>III</sup>(CF<sub>3</sub>)<sub>2</sub> and CF<sub>3</sub>• from II could not be detected computationally. Thus, in accord with the protocol presented by Hartwig and Hall,<sup>23</sup> the Gibbs initiation barrier is estimated as  $\sim \Delta H$ , i.e.  $\Delta G^{\ddagger} \sim 17.9$  kcal/mol. This barrier is significantly higher than that for  $IV \rightarrow I-H^+$  (14.4 kcal/mol),

consistent with the proposed mechanism. In addition to experimental evidence for a higher barrier for initiation versus propagation, the initiation step computes as endergonic ( $\Delta G = 3.4$  kcal/mol) and only slightly favorable after solvation to form III ligated by DMSO ( $\Delta G^{\ddagger} = -0.5$  kcal/mol).

These studies support the challenging release of CF<sub>3</sub>• from complex **II**. This is consistent with the induction period observed in both stoichiometric and catalytic reactions that start with Ni<sup>IV</sup> complex **II**. Subsequent entrance into the proposed propagative regime through the addition of CF<sub>3</sub>• to trimethoxybenzene represents a transition into a much lower energy phase of the reaction profile. In summary, these computations provide additional support for the proposed radical chain mechanism involving an energy-intensive initiation event that then provides access to a more favorable propagative regime. The Ni<sup>IV</sup>-catalyzed C–H trifluoromethylation reaction is expected to have analogous initiation and propagation as the stoichiometric variant. The reaction then turns over via the oxidation and deprotonation of **I-H**+ with the CF<sub>3</sub>+ reagent **B**.

# SUMMARY AND CONCLUSIONS

In conclusion, this study represents the first example where Ni<sup>IV</sup> intermediates are implicated spectroscopically in catalysis. Detailed experimental and computational studies of the trifluoromethylation of trimethoxybenzene mediated by complex **H** support a radical chain pathway in which this Ni<sup>IV</sup> intermediate plays a role in both the initiation and propagation regimes. Future work will investigate the use of Ni<sup>IV</sup> as a mild source of other carbon-centered radicals. Ultimately, we anticipate that the insights acquired in this study will inform the development of novel reactions involving Ni<sup>IV</sup> intermediates.

ASSOCIATED CONTENT

Experimental details, optimization tables, and complete characterization data for all new compounds. This material is available free of charge via the Internet at http://pubs.acs.org.

## **AUTHOR INFORMATION**

# **Corresponding Author**

\*mssanfor@umich.edu

#### **Notes**

The authors declare no competing financial interests.

## **ORCID**

Allan J. Canty: 0000-0003-4091-6040 Alireza Ariafard: 0000-0003-2383-6380 Melanie S. Sanford: 0000-0001-9342-9436

## **ACKNOWLEDGMENTS**

This work was supported by the National Science Foundation (NSF) Grant CHE-1111563, the Australian Research Council, and the Australian National Computing Infrastructure. We also thank Rackham Graduate School and the NSF for graduate fellowships to E.A.M, the NSF for a REU summer fellowship for S.N.N., and the NSERC for a postdoctoral fellowship for E.C. We gratefully acknowledge Dr. Jeff Kampf for X-ray crystallographic analysis of complex II, as well as funding from NSF Grant CHE-0840456 for X-ray instrumentation.

### REFERENCES

<sup>1</sup> (a) Tasker, S. Z.; Standley, E. A.; Jamison, T. F. Recent advances in homogeneous nickel catalysis. *Nature* **2014**, *509*, 299–309. (b) Ananikov, V. P. Nickel: The "spirited horse" of transition metal catalysis. *ACS Catal.* **2015**, *5*, 1964–1971. (c) Keim, W. Nickel: an element with wide application in industrial homogeneous catalysis. *Angew. Chem., Int. Ed.* **1990**, *29*, 235–244. (d) Rosen, B. M.; Quasdorf, K. W.; Wilson, D. A.; Zhang, N.; Resmerita, A.-M. Garg, N. K.; Percec, V. Nickel-catalyzed cross-coupling involving carbon–oxygen bonds. *Chem. Rev.* **2011**, *111*, 1346–1416.

<sup>2</sup> (a) J. Montgomery, in Organometallics in Synthesis: Fourth Manual, B. H. Lipschutz, Ed. (Wiley, Hoboken, NJ, 2013), pp. 319–428. (b) Hu, X. Nickel-catalyzed cross coupling of non-activated alkyl halides: a mechanistic perspective. *Chem. Sci.* **2011**, 2, 1867–1886.

<sup>3</sup> For some examples, see: (a) Tsou, T. T.; Kochi, J. K. Mechanism of oxidative addition. Reaction of nickel(0) complexes with aromatic halides. *J. Am. Chem. Soc.* **1979**, *101*, 6319–6332. (b) Laskowski, C. A.; Bungum, D. J.; Baldwin, S. M.; Del Ciello, S. A.; Iluc, V. M.; Hillhouse, G. L. Synthesis and reactivity of two-coordinate Ni(I) alkyl and aryl complexes. *J. Am. Chem. Soc.* **2013**, *135*, 18272–18275. (c) Grove, D. M.; van Koten, G.; Zoet, R. Unique stable organometallic nickel(III) complexes: syntheses and molecular structure of Ni[C<sub>6</sub>H<sub>3</sub>(CH<sub>2</sub>NMe<sub>2</sub>)<sub>2</sub>-o, o'|<sub>2</sub>I<sub>2</sub>. *J. Am. Chem. Soc.* **1983**, *105*, 1380–1381.

<sup>4</sup> For select examples of Ni<sup>IV</sup> complexes that have been isolated and studied, see: (a) Klein, H.-F.; Bickelhaupt, A.; Jung, T.; Cordier, G. Syntheses and properties of the first octahedral diorganonickel(IV) compounds. Organometallics, 1994, 13, 2557-2559. (b) Dimitrov, V.; Linden, A. A pseudotetrahedral, high-oxidation-state organonickel and compound: synthesis structure of bromotris(1-norbornyl)nickel(IV). Angew. Chem., Int. Ed. 2003, 42, 2631-2633. (c) Camasso, N. M.; Sanford, M. S. Design, synthesis, and carbon-heteroatom coupling reactions of organometallic nickel(IV) complexes. Science 2015, 347, 1218-1220. (d) Martinez, G. E.; Ocampo, C.; Park, Y. J.; Fout, A. R. Accessing pincer bis(carbene) Ni(IV) complexes from Ni(II) via halogen and halogen surrogates. J. Am. Chem. Soc. 2016, 138, 4290-4293. (e) Schultz, J. W.; Fuchigami, K.; Zheng, B.; Rath, N. P.; Mirica, L. M. Isolated organometallic nickel(III) and nickel(IV) complexes relevant to carbon-carbon bond formation reactions J. Am. Chem. Soc. 2016, 138, 12928-12934.

<sup>5</sup> (a) Bour, J.; Camasso, N. M.; Sanford, M. S. Oxidation of Ni(II) to Ni(IV) with aryl electrophiles enables Ni-mediated aryl–CF<sub>3</sub> coupling. *J. Am. Chem. Soc.* **2015**, *137*, 8034–8037. (b) Chong, E.; Kampf, J. W.; Ariafard, A.; Canty, A. J.; Sanford, M. S. Oxidatively induced C–H activation at high valent nickel. *J. Am. Chem. Soc.* **2017**, *139*, 6058–6061. (c) Zhang, C.-P.; Wang, H.; Klein, A.; Biewer, C.; Stirnat, K.; Yamaguchi, Y.; Xu, L.; Gomez-Benitez, V.; Vicic, D. A. A five-

coordinate nickel(II) fluoroalkyl complex as a precursor to a spectroscopically detectable Ni(III) species. *J. Am. Chem. Soc.* **2013**, *135*, 8141–8144.

<sup>6</sup> D'Accriscio, F.; Borja, P.; Saffon-Merceron, N.; Fustier-Boutignon, M.; Mézailles, N.; Nebra, N. C–H bond trifluoromethylation of arenes enabled by a robust, high-valent Ni<sup>IV</sup> complex. *Angew. Chem., Int. Ed.* **2017**, *56*, 12898–12902.

<sup>7</sup> The identity of Ni<sup>II</sup> product **I-H**\* was confirmed by comparing the <sup>19</sup>F NMR shift observed for the Ni<sup>II</sup> product of this reaction to the signal generated upon treatment of Ni<sup>II</sup> complex **I** with TsOH in DMSO. See SI for details

<sup>8</sup> (a) Umemoto, T.; Zhang, B.; Zhu, T.; Zhou, X.; Zhang, P.; Hu, S.; Li, Y. Powerful, thermally stable, one-pot-preparable, and recyclable electrophilic trifluoromethylating agents: 2,8-difluoro- and 2,3,7,8-tetrafluoro-S-(trifluoromethyl)bibenzothiophenium salts. *J. Org. Chem.* **2017**, 82, 7708–7719. (b) Egami, H.; Ito, Y.; Ide, T.; Masuda, S.; Hamashima, Y. Simple photo-induced trifluoromethylation of aromatic rings. *Synthesis* **2018**, *50*, 2948–2953.

<sup>9</sup> Gao, X.; Geng, Y.; Han, S.; Liang, A.; Li, J.; Zou, D.; Wu, Y.; Wu, Y. Nickel-catalyzed direct C–H trifluoromethylation of free anilines with Togni's reagent. *Org. Lett.* **2018**, *20*, 3732–3735.

<sup>10</sup> (a) Rey-Rodriguez, R.; Retailleau, P.; Bonnet, P.; Gillaizeau, I. Ironcatalyzed trifluoromethylation of enamide. *Chem. Eur. J.* **2015**, *21*, 3572–3575. (b) Jacquet, J.; Blanchard, S.; Derat, E.; Desage-El Murr, M.; Fensterbank, L. Redox-ligand sustains controlled generation of CF<sub>3</sub> radicals by well-defined copper complex. *Chem. Sci.* **2016**, *7*, 2030–2036. (c) Chang, B.; Shao, H.; Yan, P.; Qiu, W.; Weng, Z.; Yuan, R. Quinone-mediated trifluoromethylation of arenes and heteroarenes with visible light. *ACS Sustainable Chem. Eng.* **2017**, *5*, 334–341.

<sup>11</sup> Nagib, D. A.; MacMillan, D. W. C. Trifluoromethylation of arenes and heteroarenes by means of photoredox catalysis. *Nature* **2011**, *480*, 224–228.

<sup>12</sup> Ji, Y.; Brueckl, T.; Baxter, R. D.; Fujiwara, Y.; Seiple, I. B.; Su, S.; Blackmond, D. G.; Baran, P. S. Innate C-H trifluoromethylation of heterocycles. *Proc. Nat. Acad. Sci.* **2011**, *108*, 14411–14415.

<sup>13</sup> Helfferich, F. G. Chain Reactions. In *Comprehensive Chemical Kinetics*. Elsevier Science B.V.: Amsterdarm, The Netherlands 2001; Vol. 38, pp 263–297.

<sup>14</sup> (a) Seo, S.; Taylor, J. B.; Greaney, M. F. Silver-catalysed trifluoromethylation of arenes at room temperature. *Chem. Commun.* **2013**, *49*, 6385–6387. (b) Chen, S.; Feng, D.-F.; Li, D.-Y.; Liu, P.-N. Radical cyanotrifluoromethylation of isocyanides: step-econmoical access to CF<sub>3</sub>-containing nitriles, amines, and imines. *Org. Lett.* **2018**, *20*, 5418–5422. (c) Liang, A.; Han, S.; Liu, Z.; Wang, L.; Zou, D.; Wu, Y.; Wu, Y. Regioselective synthesis of N-heteroaromatic trifluoromethoxy compounds by direct O–CF<sub>3</sub> bond formation. *Chem. Eur. J.* **2016**, *22*, 5102–5106.

<sup>15</sup> Bour, J. B.; Camasso, N. M.; Meucci, E. A.; Kampf, J. W.; Canty, A. J.; Sanford, M. S. Carbon–carbon bond-forming reductive elimination from isolated nickel(III) complexes. *J. Am. Chem. Soc.* **2016**, *138*, 16105–16111.

<sup>16</sup> We investigated the possible role of the MeCN ligand on **III** by adding and removing (via vacuum) CH<sub>2</sub>Cl<sub>2</sub> from **III** several times. The resulting complex was also observed to severely inhibit the trifluoromethylation of **2** by **II**. The trifluoromethylation of **2** catalyzed by **II** performs similarly in MeCN and DMSO. These data suggest that the MeCN on **III** does not inhibit the reaction.

<sup>17</sup> (a) Tilset, M. One-electron oxidation of cyclopentadienylchromium carbonyl hydrides: thermodynamics of oxidative activation of metal-

hydrogen bonds toward homolytic and heterolytic cleavage. *J. Am. Chem. Soc.* **1992**, *114*, 2740–2741. (b) Skagestad, V.; Tilset, M. Thermodynamics of heterolytic and homolytic metal-hydrogen bond cleavage reactions of 18-electron and 17-electron group 6 hydridotris(pyrazolyl)borate metal hydrides. *J. Am. Chem. Soc.* **1993**, *115*, 5077–5083. (c) Tilset, M.; Hamon, J.-R.; Hamon, P. Relative M–X bond dissociation energies in 16-, 17- and 18-electron organotransition-metal complexes (X = halide, H). *Chem. Commun.* **1998**, 765–766.

<sup>18</sup> Connelly, N. G.; Geiger, W. E. Chemical redox agents for organometallic chemistry. *Chem. Rev.* **1996**, *96*, 877–910.

 $^{19}$  Attempts to utilize Cp<sub>2</sub>Co and TsOH to initiate the catalytic reaction did not result in higher yields, see SI for details.

<sup>20</sup> Bour, J. R.; Ferguson, D. M.; McClain, E. J.; Kampf, J. W.; Sanford, M. S. Connecting organometallic Ni(III) and Ni(IV): Reactions of carbon-centered radicals with high-valent organonickel complexes. *J. Am. Chem. Soc.* **2019**, *141*, 8914–8920.

<sup>21</sup> Frisch, M. J.; Trucks, G. W.; Schlegel, H. B. Scuseria, G. E.; Robb, M. A.; Cheeseman, J. R.; Scalmani, G.; Barone, V.; Mennucci, B.; Petersson, G. A.; Nakatsuji, H.; Caricato, M.; Li, X.; Hratchian, H. P.; Izmaylov, A. F.; Bloino, J.; Zheng, G.; Sonnenberg, J. L.; Hada, M.; Ehara, M.; Toyota, K.; Fukuda, R.; Hasegawa, J.; Ishida, M.; Nakajima, T.; Honda, Y.; Kitao, O.; Nakai, H.; Vreven, T.; Montgomery, Jr. J. A.; Peralta, J. E.; Ogliaro, F.; Bearpark, M.; Heyd, J. J.; Brothers, E.; Kudin, K. N.; Staroverov, V. N.; Kobayashi, R.; Normand, J.; Raghavachari, K.; Rendell, A.; Burant, J. C.; Iyengar, S. S.; Tomasi, J.; Cossi, M.; Rega, N.; Millam, J. M.; Klene, M.; Knox, J. E.; Cross, J. B.; Bakken, V.; Adamo, C.; Jaramillo, J.; Gomperts, R.; Stratmann, R. E.; Yazyev, O.; Austin, A. J.; Cammi, R.; Pomelli, C.; Ochterski, J. W.; Martin, R. L.; Morokuma, K.; Zakrzewski, V. G.; Voth, G. A.; Salvador, P.; Dannenberg, J. J.; Dapprich, S.; Daniels, A. D.; Farkas, O.; Foresman, J. B.; Ortiz, J. V.; Cioslowski, J.; and Fox, D. J. *Gaussian 09*, revision A.02; Gaussian, Inc.; Wallingford CT, 2009.

Lee, C. T.; Yang, W. T.; Parr, R. G. Development of the Colle-Salvetti correlation-energy formula into a functional of the electron density. *Phys. Rev. B* 1988, *37*, 785–789. (b) Miehlich, B.; Savin, A.; Stoll, H.; Preuss, H. Results obtained with the correlation energy density functionals of becke and Lee, Yang and Parr. *Chem. Phys. Lett.* 1989, *157*, 200–206. (c) Becke, A. D. Density-functional thermochemistry. III. The role of exact exchange. *J. Chem. Phys.* 1993, *98*, 5648–5652.
(a) Hartwig, J. F.; Cook, K. S.; Hapke, M.; Incarvito, C. D.; Fan, Y.; Webster, C. E.; Hall, M. B. Rhodium boryl complexes in the catalytic, terminal functionalization of alkanes. *J. Am. Chem. Soc.* 2005, *127*, 2538–2552. (b) Wei, C. S.; Jiménez-Hoyos, C. A.; Videa, M. F.; Hartwig, J. F.; Hall, M. B. Origins of the selectivity for borylation of primary over secondary C–H bonds catalyzed by Cp\*-Rhodium complexes. *J. Am. Chem. Soc.* 2010, *132*, 3078–3091.

TOC Graphic: